Carnegie Observatories Astrophysics Series, Vol. 1:
Coevolution of Black Holes and Galaxies, 2004
ed. L. C. Ho (Pasadena: Carnegie Observatories,
http://www.ociw.edu/ociw/symposia/series/symposium1/proceedings.html)

Photon-trapping Effects in Supercritical Accretion Flows onto Black Holes

K. OHSUGA and S. MINESHIGE
Yukawa Institute for Theoretical Physics, Kyoto University, Japan

Abstract

We investigate the spectral energy distribution (SED) in the super-critical disk accretion flows around the black holes, by solving the multi-frequency radiation transfer as well as the energy equations of radiation and gas. Here, special attention is paid on the photon-trapping effects, that is, photons diffuse towards not only the vertical direction but also radial direction with the accreting gas.

By the enhanced photon-trapping, when $L \geq 3L_{\rm E}$, the peak frequency of the SED tends to decrease in spite of increase of mass-accretion rate. Since the high-energy photons are generated near the equatorial plane, they are more effectively trapped in the flow than the low-energy ones and the SED shifts to lower-energy side.

In comparison with the observational data in the X-ray H-R diagram, we found that the black hole of IC 342 S1, which is an ultraluminous X-ray source (ULXs), is considerably massive, $\sim 100M_{\odot}$, and the time variation of IC 342 S1 data can be explained only by the modulation of the mass-accretion rate.

1.1 Introduction

There seem to be several possible sites of super-critical accretion flow, i.e., micro-quasars (Honma, Kato, & Matsumoto 1991; Yamaoka, Ueda, & Inoue 2001), ULXs (Okada et al. 1998; Colbert & Mushotzky 1999; Mizuno et al. 1999; Makishima et al. 2000; Watarai et al. 2000; Revnivtsev et al. 2002), narrow-line Seyfert 1 galaxies (Mineshige et al. 2000), quasars (Collin et al. 2002), and Gamma-ray bursts (Narayan, Piran, & Kumar 2001; Kohri & Mineshige 2002). When the mass-accretion rate, $\dot{M}$, exceeds the critical value, $L_{\rm E}/c^2$, a photon trapping plays an important role within the trapping radius, $r_{\rm trap} \sim (\dot{M}c^2/L_{\rm E})\left(H/r\right) r_{\rm g}$, where $L_{\rm E}$ is the Eddington luminosity, H is the disk-half thickness, r is the radius, and $r_{\rm g}$ is the Schwarzschild radius (Ohsuga et al. 2002), since the radiative diffusion timescale is longer than the accretion timescale, there. Thus, the radiation energy is trapped in the flow and advected inward without being immediately radiated away.

The standard-disk model, which was proposed by Shakura & Sunyaev (1973), has had some success in describing optically thick flow structure in luminous objects. However, its treatment is only justified when the mass-accretion rate is less than the critical mass-accretion rate. Since an advective energy transport is considered in the slim-disk model proposed by Abramowicz et al. (1988), this model is believed to be the solution of the super-critical accretion flow (Kato, Fukue, & Mineshige 1998). However, it is shown in

Ohsuga et al. (2002) that the photon-trapping effects are not accurately treated in the slim-disk approach.

In this work, by solving multi-frequency radiation transfer, we investigate the SED as well as the luminosity of the optically-thick black-hole accretion flows with the super-critical mass-accretion rate. Here, we pay attention to the photon-trapping effects. Comparing with the observational data of ULXs, we also discuss about the importance of the photon trapping in real objects.

Throughout this study, we employ a simple accretion flow model and solve multi-frequency radiation transfer equations coupled with energy equations of gas and radiation. The accretion model and basic equations are shown in Ohsuga, Mineshige, & Watarai (2003).

1.2 Results

1.2.1 Luminosity and spectral energy distribution

We plot the luminosity against the mass-accretion rate in Figure 1.1, where the luminosity and mass-accretion rate are normalized by the Eddington luminosity and the critical mass-accretion rate, respectively. The luminosity should increase along the dashed line, if the energy-conversion efficiency, $\eta \equiv \dot{M}c^2/L$, is constant. However, it is found that the energy-conversion efficiency decreases with increase in the mass-accretion rate at $L \geq L_{\rm E}$ due to the photon trapping. We also see that the larger ε_{100} is, the less becomes luminosity at high mass-accretion rates, see $\dot{m} \gg 10$, where ε_{100} is dimensionless parameter representing the aspect ratio, H/r, at $\dot{m} = 100$. Since the radiative diffusion timescale is proportional to the disk half thickness, the photon-trapping effects are more conspicuous in the case of large ε_{100}.

As shown in Figure 1.1, the resultant luminosity for $\varepsilon_{100} = 0.5$ is insensitive to the mass-accretion rate when $\dot{m} > 50$. However, the SED drastically change with $\dot{m}$. In Figure 1.2, we plot the variations of SED with change in $\dot{m}$ for $\varepsilon_{100} = 0.5$. The peak frequency of the SED increases as the mass-accretion rate increases up to $\dot{m} = 50$. However, when $\dot{m}$ is larger than 50, the peak frequency decreases with increase of the mass-accretion rate. This is due to the photon-trapping effects. Since the high-energy photons arise from deeper inside the disk, they tend to be more effectively trapped in the flow than the low-energy ones. Thus, the emergent SED shift towards lower-energy side when the normalized mass-accretion rate, $\dot{m}$, exceeds some critical value.

1.2.2 X-ray H-R diagram

Next, following Watarai et al. (2000). we fit the calculated spectra to get a fitting parameter, $kT_{\rm in}$. Here, we adopt the photon energy range between 0.1keV and 5keV for the fitting, but we should keep in mind that the fitting results depend on the adopted energy range, in which the fitting is made. We plot the resultant $kT_{\rm in}$ in comparison with the observational data in the X-ray H-R diagram (see Figure 1.3).

As shown in Figure 1.3, the fitting parameter, $kT_{\rm in}$, for the case of $M = 10M_\odot$ and $\varepsilon_{100} = 0.17$ (filled squares) increases as the mass-accretion rate increases. In the case of $\varepsilon_{100} = 0.5$ (filled circles), in contrast, $T_{\rm in}$ decreases with increase of $\dot{m}$ when $\dot{m} > 30$. This is due to very efficient photon-trapping effects, by which the emergent SED shifts towards the lower-energy side, leading to a decrease in $kT_{\rm in}$. (As shown in Figure 1.1, the photon-trapping effects are more conspicuous in the accretion flow with larger ε_{100}.)

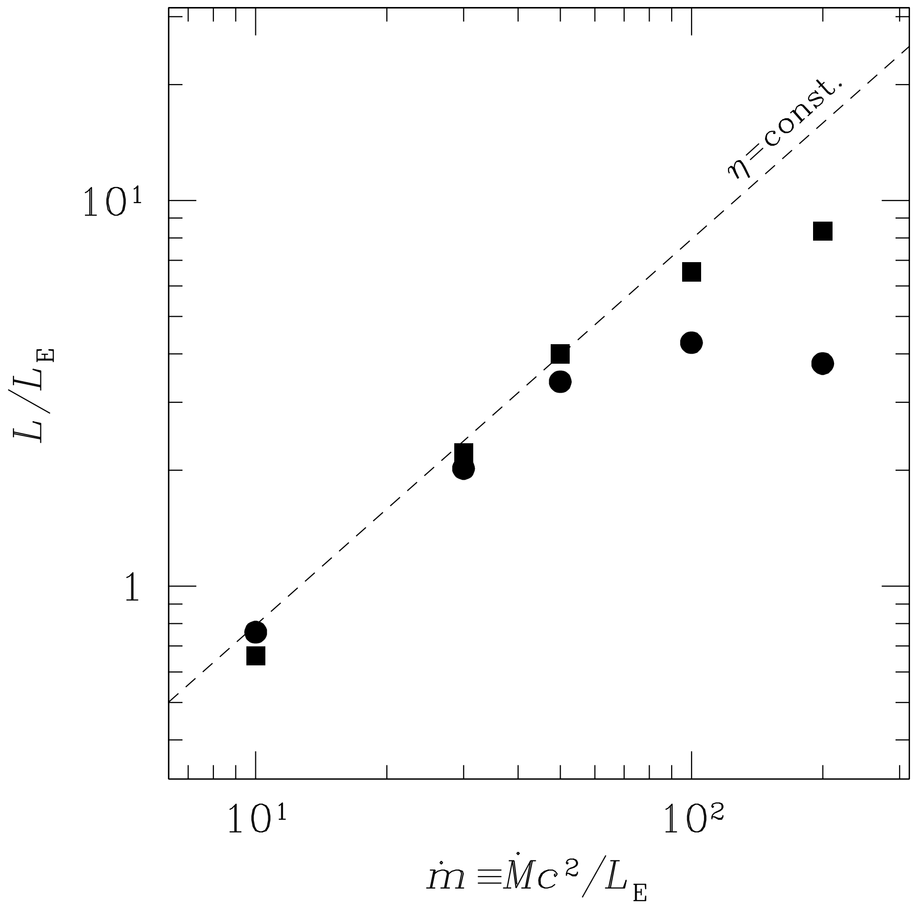

Fig. 1.1. Total disk luminosity as a function of the mass-accretion rate. The circles and squares represent the cases with $\varepsilon_{100} = 0.5$ and 0.17, respectively, where ε_{100} is a dimensionless parameter defined as $\varepsilon_{100} \equiv (H/r)/(\dot{m}/100)$.

In this Figure, we found that the case of $\varepsilon_{100} = 0.17$ (filled squares) coincides best with the observational results of M81 S-6. The behavior for the case of $\varepsilon_{100} = 0.5$ (filled circles) is contrary to the observed trend. Therefore, we can conclude that the cases with $\varepsilon_{100} = 0.5$ can be ruled out, that is, the photon-trapping effects should only moderately appear in the accretion flow of ULXs. This conclusion is supported by the fitting to the IC 342 S1 data, which is also well reproduced by the cases with $\varepsilon_{100} = 0.17$, if the black-hole mass is scaled up to $M = 100M_\odot$ (see open squares).

From the fitting to the IC 342 S1 data, we find that the black hole in IC 342 S1 is considerably massive, $\sim 100M_\odot$. Note that Watarai, Mizuno, & Mineshige (2001) estimated the mass to be $\sim 30M_\odot$ based on the slim-disk model. Scatters of IC 342 S1 data in the H-R diagram is understood in term of the variation of the mass-accretion rate according to

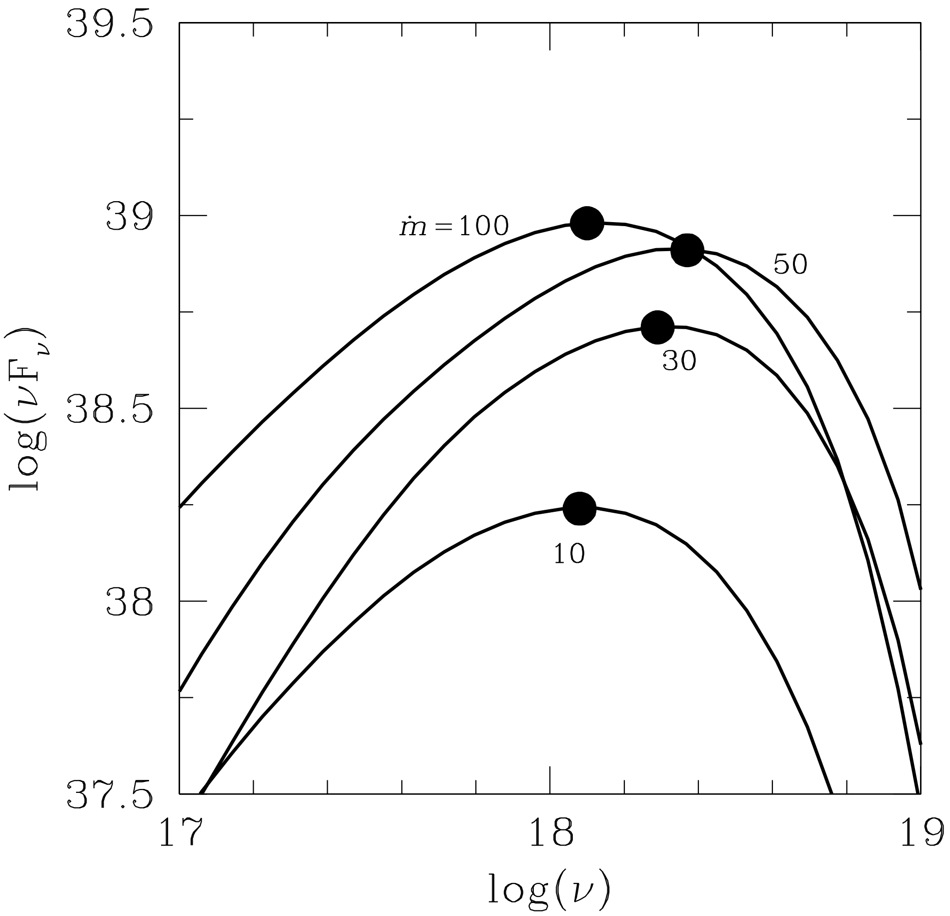

Fig. 1.2. The SED for $\varepsilon_{100} = 0.5$ for different mass-accretion rates, $\dot{m}$ = 10, 30, 50, and 100.

our model, whereas the black-hole mass should change to fit the observation if we adopt the standard-disk model, which is, of course, unreasonable. Our model is certainly preferable.

1.3 Conclusions

We have investigated the SED in the super-critical accretion flow, with special attention on the photon-trapping effects, by solving the multi-frequency radiation transfer and the energy equations of gas as well as radiation.

For $L \geq 3L_{\rm E}$ ($\dot{m} \geq 50$), the photon-trapping effects are substantial and, then, the high-energy photons are more efficiently trapped in the flow than the low-energy ones, since the former arise near the equatorial plane. Thus, the SED shifts towards the lower-energy side as $\dot{m}$ increases so that the photon-trapping effects can be enhanced.

By comparing with the observational data of ULXs in the X-ray H-R diagram, we found that the photon-trapping effects would only moderately appear in the accretion flow of

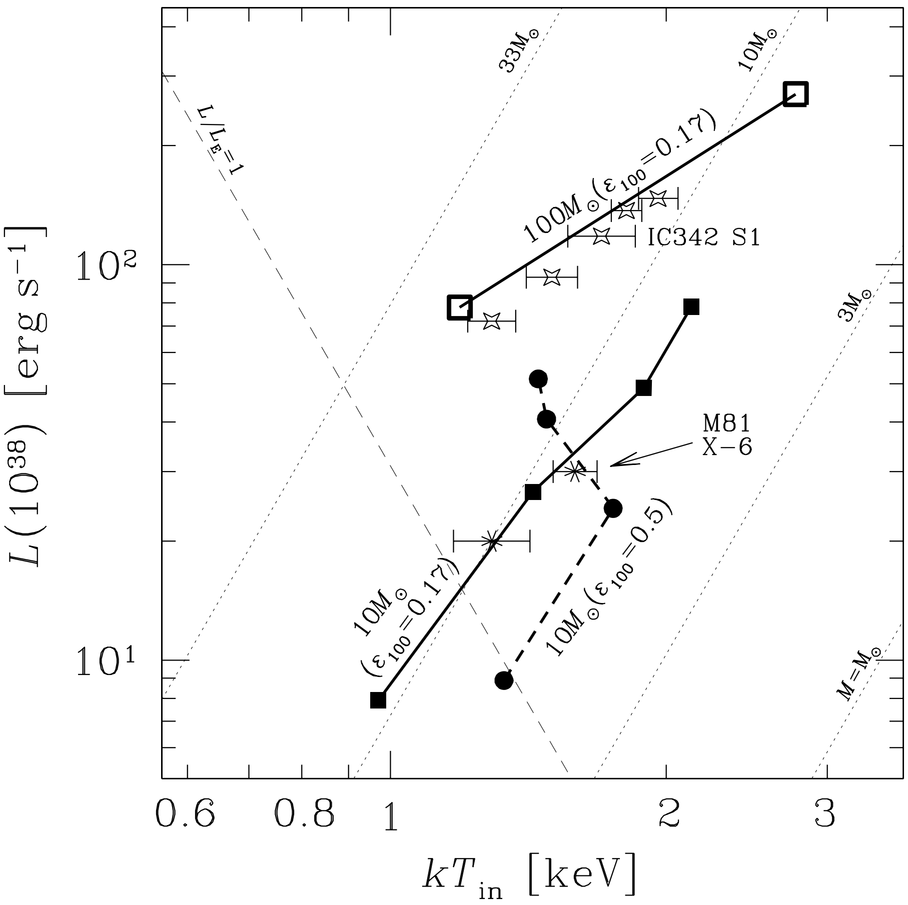

Fig. 1.3. X-ray H-R diagram. The filled circles and filled squares indicate numerical results for $\varepsilon_{100} = 0.5$ and 0.17, respectively, with different mass-accretion rates, $\dot{m} = 10$, 30, 50, and 100 from the bottom to the top. The open squares represent the results for $\varepsilon_{100} = 0.17$, but the black-hole mass is $100M_\odot$. We plot only results of $\dot{m} = 10$ and 30 in the case of $M = 100M_\odot$. The dotted lines correspond to the cases of the standard-disk model with different black-hole mass. Based on the standard-disk model, the luminosity becomes the Eddington luminosity on the thin dashed line.

ULXs. We can explain the observed time variations of IC 342 S1 on the X-ray H-R diagram in terms of $\dot{m}$ modulation. The estimated black-hole mass is $M \sim 100M_\odot$, which is greater than the previous estimate based on the slim-disk model (Watarai, Mizuno, & Mineshige 2001).

References

Abramowicz, M. A., Czerny, B., Lasota, J. P., & Szuszkiewicz, E. 1988, ApJ, 332, 646
Colbert, E. J. M., & Mushotzky, R. F. 1999, ApJ, 519, 89

Collin, S., et al. 2002, A&A, 388, 771
Honma, F., Kato, S., & Matsumoto, R. 1991, PASJ, 43, 147
Kato, S., Fukue, J., & Mineshige, S. 1998, Black-Hole Accretion Disks (Kyoto: Kyoto Univ. Press)
Kohri, K., & Mineshige, S. 2002, ApJ, 577, 311
Makishima, K., et al. 2000, ApJ, 535, 632
Mineshige, S., Kawaguchi, T., Takeuchi, M., & Hayashida, K. 2000, PASJ, 52, 499
Mizuno, T., Ohnishi, T., Kubota, A., Makishima, K., & Tashiro, M. 1999, PASJ, 51, 663
Narayan, R., Piran, T., & Kumar, P. 2001, ApJ, 557, 949
Ohsuga, K., Mineshige, S., Mori, M., & Umemura, M. 2002, ApJ, 574, 315
Ohsuga, K., Mineshige, S., & Watarai, K. 2003, ApJ, 596, 429
Okada, K., Dotani, T., Makishima, K., Mitsuda, K., & Mihara, T. 1998, PASJ, 50, 25
Revnivtsev, M., Gilfanov, M., Churazov, E., & Sunyaev, R. 2002, A&A, 391, 1013
Shakura, N. I., & Sunyaev, R. A. 1973, A&A, 24, 337
Watarai, K., Fukue, J., Takeuchi, M., & Mineshige, S. 2000, PASJ, 52, 133
Watarai, K., Mizuno, T., & Mineshige, S. 2001, ApJ, 549, L77
Yamaoka, K., Ueda, Y., Inoue, H. 2001, in New Century of X-Ray Astronomy, ed. H. Inoue & H. Kunieda (San Francisco: ASP), 426